

Atropisomerism in Amidinoquinoxaline *N*-Oxides: Effect of the Ring Size and Substituents on the Enantiomerization Barriers

Jimena E. Díaz,^{†,‡} Nicolas Vanthuyne,[†] H  l  ne Rispaud,[†] Christian Roussel,^{*,†} Daniel Vega,[§] and Liliana R. Orelli^{*,‡}

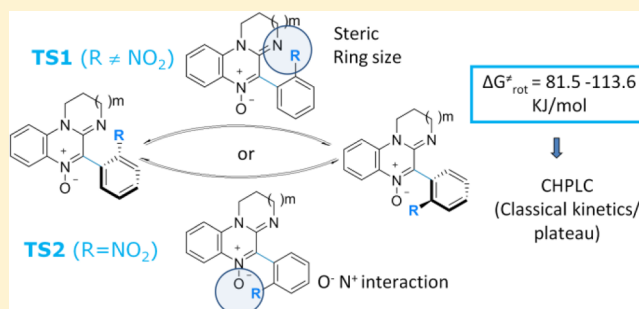
[†]Aix Marseille Universit  , Centrale Marseille, CNRS, iSm2 UMR 7313, 13397, Marseille, France

[‡]Departamento de Qu  mica Org  nica, Facultad de Farmacia y Bioqu  mica, Universidad de Buenos Aires, CONICET. Jun  n 956, (1113) Buenos Aires, Argentina

[§]Departamento F  sica de la Materia Condensada, Gerencia de Investigaci  n y Aplicaciones, Comisi  n Nacional de Energ  a At  mica y ECyT, Universidad Nacional de General San Mart  n, Av. Gral. Paz 1499, (1650) San Mart  n, Buenos Aires, Argentina

Supporting Information

ABSTRACT: The atropisomerism of novel 2,3-dihydro-1*H*-pyrimido[1,2-*a*]quinoxaline 6-oxides **1** bearing dissymmetric (*ortho*-substituted) 5-aryl residues and the homologous 1,2-dihydroimidazo[1,2-*a*]quinoxaline 5-oxides **2** was investigated. The existence of a chiral axis was demonstrated for compound **1a** by X-ray diffraction and by DFT calculations of the ground state geometry. The resolution of the atropisomeric enantiomers on chiral stationary phases is reported. The barriers to enantiomerization were determined by off-line racemization studies and/or by treatment of the plateau-shaped chromatograms during chromatography on chiral support. A clear ring size effect was evidenced. In all cases, six-membered amidine derivatives **1** showed higher barriers than the corresponding lower homologues **2**, which also display lower sensitivity to the substituent size. Transition states for the interconversion of the atropisomers were located using DFT calculations, and involved the interaction of the *ortho* substituent with the formally sp² nitrogen in the amidine moiety. In contrast, in the most favored enantiomerization transition state of the 2-nitro derivative the *ortho* substituent is close to the *N*-oxide group.



INTRODUCTION

2,3-Dihydro-1*H*-pyrimido[1,2-*a*]quinoxaline *N*-oxides represent a heterocyclic core of interest due to their pharmacological properties. Some suitably substituted derivatives possess antineoplastic activity,¹ especially against hypoxic tumors. Other pyrimidoquinoxaline 6-oxides have been employed as antiamebic² and antianaerobic agents.³ As part of our research on nitrogen heterocycles, we reported a novel methodology for their synthesis,⁴ and investigated some of their chemical,⁵ spectroscopic,⁶ and pharmacological⁷ properties. We recently demonstrated their ability to act as spin traps.⁸ In particular, derivatives containing a dissymmetrical (*ortho* substituted) 5-aryl substituent show diastereotopicity of the CH₂ signals in their ¹H NMR spectra.⁶ Such behavior indicates the presence of a chiral axis (C5-aryl), which entails the existence of two atropisomers. Atropisomeric compounds have been described as drugs⁹ and chiral selectors.¹⁰ The axial chirality in natural compounds has been reviewed.¹¹ Atropisomeric biaryls are widely employed as chiral ligands, reagents, and catalysts in stereoselective reactions.¹² In particular, atropisomerism in heterocyclic compounds has recently been reviewed.¹³

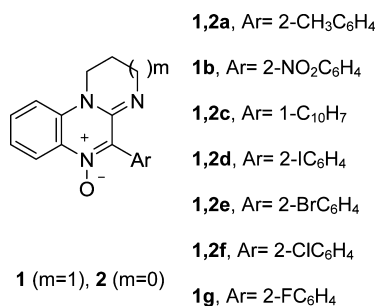
Attempts at studying the enantiomerization of atropisomeric 2,3-dihydro-1*H*-pyrimido[1,2-*a*]quinoxaline *N*-oxides by means of dynamic NMR were unsuccessful as the *N*-methylene signals did not display the line broadening typical of an exchange process, even when the sample was heated at +120 °C, indicating that the enantiomerization barrier must be higher than 80 kJ mol⁻¹.¹⁴ As part of ongoing research on atropisomerism¹⁵ and, in particular, on atropisomeric amidines and related compounds,¹⁶ we investigate here the chiral separation and enantiomerization barriers of a series of atropisomeric 2,3-dihydro-1*H*-pyrimido[1,2-*a*]quinoxaline *N*-oxides **1** and the homologous 1,2-dihydroimidazo[1,2-*a*]quinoxaline 5-oxides **2**. Analysis of both experimental and theoretical data show some general trends regarding substituent effects and amidine ring size sensitivity of the enantiomerization barriers.

Received: November 17, 2014

Published: January 13, 2015

RESULTS AND DISCUSSION

The structure of amidinoquinoxaline *N*-oxides **1,2** under study is shown in Scheme 1. We previously described the synthesis of amidinoquinoxaline *N*-oxides **1a,d,e,f** and **2a,e**.^{6,8} The remaining compounds were synthesized by our previously reported method.⁴

Scheme 1. General Structure of Amidinoquinoxaline *N*-Oxides

DFT calculations (B3LYP/6-31+G(d,p) method) applied to the *o*-tolyl derivative **1a** indicate that the dihedral angle comprising the chiral axis (C4–C5–C1'–C2') has a value of 113.8°, thus entailing the existence of two enantiomeric forms (Figure 1). A single-crystal X-ray diffraction of **1a** confirms the

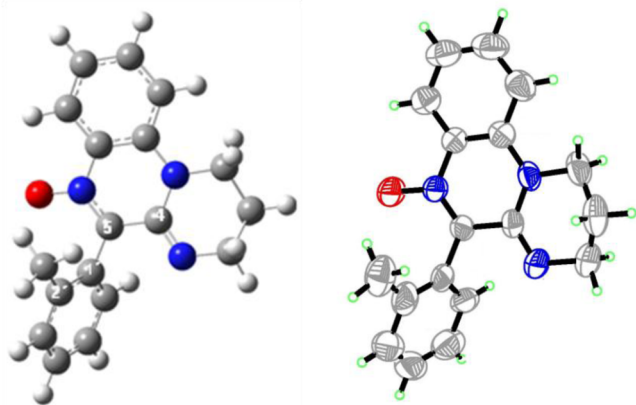


Figure 1. B3LYP/6-31+G(d,p) computed structure of the M atropisomer of **1a** (left). Experimental structure as obtained by X-ray diffraction (right).

theoretical results. The geometrical parameters determined in the solid state are quite similar to those computed for the isolated molecule; in particular, the dihedral angle mentioned has a very similar value (112.4°). The experimental X-ray structure of **1a** (M enantiomer) is also displayed in Figure 1.

Interestingly, *ortho* substitution in the aryl group also brings about a significant change in the EI mass spectra of amidinoquinoxalines. In unsubstituted or *para* substituted pyrimidoquinoxaline *N*-oxides **1h,i** the base peak arises from H[•] loss, according to the proposed mechanism depicted in Figure 2 (left).¹⁷ In contrast, the base peak for atropisomeric *ortho* substituted amidinoquinoxalines **1a,f** and **2d,f** results from loss of the aryl substituent G[•] (Figure 2, right). In compounds bearing a 2-naphthyl group (**1,2c**) this fragmentation is not possible and the base peaks arise, respectively, from loss of OH[•] (*m/z* = 310)¹⁸ or H[•] (*m/z* = 312).

Compounds **1,2** were submitted to HPLC on chiral support using a screening unit equipped with 10 commercially available chiral columns and chiroptical detection (CD at 254 nm). Our objective was to find suitable conditions for the isolation of the enantiomers in order to measure their enantiomerization barriers. In most of the cases, several columns allowed the baseline separation of the enantiomers using a classical mobile phase composed of hexane and ethanol. Compounds **1b,g** underwent interconversion during the separation process, displaying typical plateau shape chromatograms.¹⁹ Selected examples are given in Table 1.

Regarding their stereostability, compounds **1,2** were sorted into three groups. The first one (compounds **1c–f**, **2d,e**) displayed well separated peaks corresponding to both atropisomers, and thus their racemization could be monitored by the off-column method. For the second group (compounds **1b,g**, **2a**), plateau-shaped chromatograms were obtained due to on-column racemization, indicating a lower interconversion barrier. This behavior is exemplified in Figure 3 for compound **1b**.

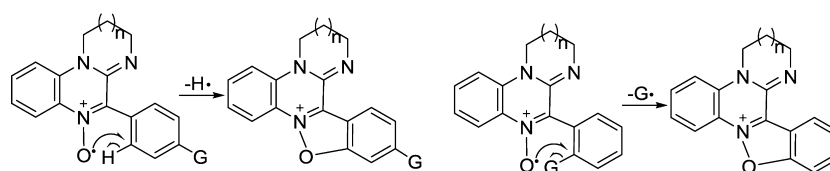
Finally, the third group comprised compounds with intermediate barriers (**1a**, **2c,f**), which gave baseline separation or plateau-shaped chromatograms according to the temperature. All the barriers to enantiomerization were determined using either classical off-line racemization kinetics²⁰ or the equation developed by Trapp and Schurig in the case of a plateau,²¹ and are collected in Table 2. The enantiomerization rates correspond to the racemization rates divided by a factor of 2.

In order to assess the influence of steric effects on the enantiomerization barriers of pyrimidoquinoxaline *N*-oxides **1**, their values were plotted vs the steric parameters developed for substituted biaryls (*B* values),²² whenever available (Figure 4).

It can be observed that derivatives **1a,d–g** show a very good linear correlation, while the barrier of compound **1b** is lower than expected. Such behavior suggests, in principle, an alternative enantiomerization path involving a stabilizing interaction between the N(+) of the nitro group and the oxygen of the *N*-oxide in the transition state.

A comparative analysis of the barriers reported in Table 2 shows that *N*-oxides **2** containing a five-membered amidine ring show lower enantiomerization barriers than the corresponding homologues **1**. This could be due mainly to differences in the external bond angles of the amidine moieties, which are decisive in determining the resulting distances between interacting groups. An interesting point is that this ring size effect also involves a higher sensitivity of the barrier to the size and nature of the *ortho* substituent in the six-membered than in the five-membered rings. In Figure 5, a plot of the enantiomerization barriers of both types of compounds is presented, showing that the slopes are >1 when comparing the six-membered with the five-membered rings. Furthermore, in the set of halogens the slope is significantly higher than for the hydrocarbon substituents (methyl and naphthyl). Such differences would suggest that changes in the geometry between five- and six-membered amidine rings would additionally determine subtle variations in the hybridization of the formally sp² nitrogen which interacts with the *ortho* substituent in the transition states. In fact, previous studies have shown that 1,2-diaryl-limidazolines are considerably less basic than the homologous tetrahydropyrimidines.^{23,24}

In order to further investigate the path involved in the enantiomerization process under study, the two possible



1h: G=H, n=1. $[M-H]^+$, $m/z=276$ (BP);

1i: G=OCH₃, n=1. $[M-H]^+$, $m/z=306$ (BP);

1a: G=CH₃, n=1. $[M-G]^+$, $m/z=276$ (BP); $[M-H]^+$, $m/z=290$ (<5%);

1f: G=Cl, n=1. $[M-G]^+$, $m/z=276$ (BP); $[M-H]^+$, $m/z=310$ (<5%);

2d: G=I, n=0. $[M-G]^+$, $m/z=262$ (BP); $[M-H]^+$, $m/z=388$ (ND);

2f: G=Cl, n=0. $[M-G]^+$, $m/z=262$ (BP); $[M-H]^+$, $m/z=296$ (ND).

Figure 2. Proposed fragmentation pathways leading to the base peaks in the mass spectra (EI) of amidinoquinoxalines **1a,f,h,i**, and **2d,f**.

Table 1. Selected Chiral HPLC Chromatographic Data for Atropisomers **1a–g**, **2a–f**

compd.	Ar	n	column	eluent	k_1	k_2	α	first eluted ^a
1a	2-CH ₃ C ₆ H ₄	1	Chiralcel OJ-H (25 °C)	hexane:ethanol 50:50	2.04	5.12	2.51	(-)
			Chiralcel OD-H (25 °C)	hexane:ethanol 50:50	0.84	1.81	2.16	(+)
			Chiralcel OD-H	hexane:ethanol 50:50	Plateau at 50 °C			
1b	2-NO ₂ C ₆ H ₄	1	Chiralpak IB	hexane:ethanol 50:50	Plateau at 5, 10, 15, and 20 °C			
1c	1-C ₁₀ H ₇	1	Chiralpak AS-H	hexane:ethanol 50:50	1.64	4.04	2.47	(-)
1d	2-IC ₆ H ₄	1	Chiralcel OJ-H (25 °C)	hexane:ethanol 50:50	5.41	8.78	1.62	(-)
1e	2-BrC ₆ H ₄	1	Chiralcel OJ-H (25 °C)	hexane:ethanol 50:50	4.99	9.15	1.84	(-)
1f	2-ClC ₆ H ₄	1	Chiralcel OJ-H (25 °C)	hexane:ethanol 50:50	4.18	8.16	1.95	(-)
1g	2-FC ₆ H ₄	1	Chiralcel OD-H	methanol	Plateau at 7 °C			
2a	2-CH ₃ C ₆ H ₄	0	Chiralcel OJ-H (25 °C)	hexane:ethanol 50:50	3.77	4.44	1.18	(-)
			Chiralpak AD-H (25 °C)	hexane:ethanol 50:50	1.77	2.20	1.27	(-)
			Chiralpak AD-H	hexane:ethanol 50:50	Plateau at 35 °C			
2c	1-C ₁₀ H ₇	0	Chiralcel OJ-H (25 °C)	hexane:ethanol 50:50	3.87	7.55	1.95	(+)
			Chiralcel OJ-H	hexane:ethanol 50:50	Plateau at 40 °C			
2d	2-IC ₆ H ₄	0	Chiralpak AS-3 (25 °C)	hexane:ethanol 50:50	0.96	1.22	1.27	(+)
2e	2-BrC ₆ H ₄	0	Chiralpak AD-H (25 °C)	hexane:ethanol 50:50	2.25	4.37	1.94	(-)
2f	2-ClC ₆ H ₄	0	Chiralpak AD-H (25 °C)	hexane:ethanol 50:50	2.30	3.61	1.57	(-)
			Chiralpak AD-H	hexane:ethanol 50:50	Plateau at 50 °C			

^aThe sign of the first eluted enantiomer reported in Table 2 is the sign given by the circular dichroism detector at 254 nm in the mobile phase.

transition states for the interconversion of the atropisomers of compound **1a** were calculated using the DFT B3LYP/6-31+G(d,p) method. Their geometries and relative energies are displayed in Figure 6.

It can be seen that in the lower energy transition state (TS1), the *ortho* substituent passes near the formally sp² amidine nitrogen. Similar results (TS1) were obtained for compounds **1c,e–g**, **2a,c,e,f**. The calculated enantiomerization barriers are reported in Table 3.

Compound **1b** represents an exception, since the transition state in which the nitro group crosses over the *N*-oxide moiety (TS2, Figure 7) is favored. This behavior may be explained considering a stabilizing N⁺...O⁻ interaction between the electron deficient nitrogen atom within the nitro group and the electron-rich oxygen of the *N*-oxide moiety in the transition state. A related type of donor–acceptor interaction is known to operate in other heterocyclic compounds bearing *ortho*-nitrophenyl groups.²⁵

CONCLUSIONS

A novel class of atropisomers derived from the amidinoquinoxaline *N*-oxide core was investigated. The chirality of the compounds was demonstrated both by X-ray diffraction and theoretical calculations. A screening of different chiral stationary phases and chromatographic conditions allowed for the baseline separation of most of the compounds. Rotational barriers were determined either by classical off-line racemization kinetics or by deconvolution of the corresponding plateau-shaped chromatograms, according to their magnitude. In three examples, both methods gave similar results. The barriers were also calculated using the DFT B3LYP/6-31+G(d,p) method and a good correlation with the experimental values was in general attained. With the exception of nitroderivative **1b**, the calculated transition state for the interconversion of the atropisomers involves the interaction of the *ortho* substituent with the formally sp² nitrogen of the amidine ring. Six-membered amidine derivatives showed in all cases higher rotational barriers than the corresponding five-membered homologues. Interestingly, the ring size effect also modifies

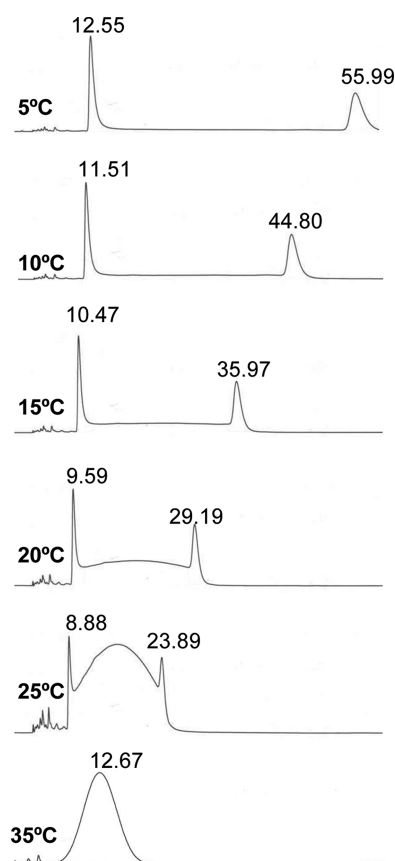


Figure 3. Evolution of the chromatographic profile of **1b** atropisomers as a function of temperature: Chiralpak IB, hexane/ethanol (50:50), 1 mL/min, UV detection at 254 nm.

the sensitivity of the barriers to the substituent size, which is comparatively higher for six-membered amidine derivatives. The observed differences between both groups of compounds were rather unexpected, as the structural variation occurs at a considerable distance from the stereogenic axis. Finally, nitro derivative **1b** is the only compound in which in the rotation transition state the *ortho* substituent crosses over the *N*-oxide moiety.

Table 2. Barriers to Rotation for Compounds **1a–g**, **2a–f**

compd	Ar	<i>n</i>	rotational barrier (kJ/mol)	<i>T</i> (°C)	solvent	<i>t</i> _{1/2} (min)
1a	2-CH ₃ C ₆ H ₄	1	99.2 ^a	30	ethanol	114
			99.8 ^b	50	hexane:ethanol 50:50	11.5
1b	2-NO ₂ C ₆ H ₄	1	87.1 ^b	25	hexane:ethanol 50:50	1.7
1c	1-C ₁₀ H ₇	1	105.1 ^a	40	ethanol	300
1d	2-IC ₆ H ₄	1	113.6 ^a	78	ethanol	62
1e	2-BrC ₆ H ₄	1	110.1 ^a	50	ethanol	527
1f	2-ClC ₆ H ₄	1	104.6 ^a	50	ethanol	70
1g	2-FC ₆ H ₄	1	81.5 ^b	7	methanol	1.5
2a	2-CH ₃ C ₆ H ₄	0	95.3 ^b	35	hexane:ethanol 50:50	13
			100.3 ^a	30	ethanol	175
2c	1-C ₁₀ H ₇	0	100.3 ^b	40	hexane:ethanol 50:50	48
			107.5 ^a	50	ethanol	202
2e	2-BrC ₆ H ₄	0	106.8 ^a	40	ethanol	662
2f	2-ClC ₆ H ₄	0	102.3 ^a	30	ethanol	383
			101.2 ^b	50	hexane:ethanol 50:50	20

^aMethod: off-column racemization. ^bMethod: online plateau treatment.

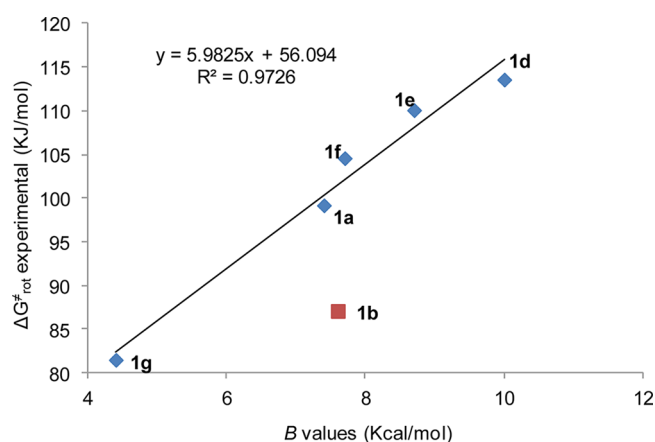


Figure 4. Experimental barriers vs substituent *B* values for compounds **1a, b, d–g**.

EXPERIMENTAL SECTION

Synthesis. Melting points were determined with a capillary apparatus and are uncorrected. ¹H and ¹³C NMR spectra were recorded on a 500 MHz spectrometer, using deuteriochloroform as the solvent. Chemical shifts are reported in parts per million (ppm) relative to TMS as an internal standard. Coupling constants are reported in Hz. D₂O was employed to confirm exchangeable protons (ex). Splitting multiplicities are reported as singlet (s), broad signal (bs), doublet (d), double doublet (dd), doublet of double doublets (ddd), triplet (t), triple doublet (td), pentet (p), and multiplet (m). HRMS (ESI) were performed with a MicroTOF-Q spectrometer.

Reagents, solvents, and starting materials were purchased from standard sources and purified according to literature procedures.

Synthesis of 5-aryl-2,3-dihydro-1*H*-pyrimido[1,2-*a*]quinoxaline 6-oxides **1** and 1,2-dihydroimidazo[1,2-*a*]quinoxaline 5-oxides **2**.

A mixture of the corresponding aminoamide **3** or **4** (1 mmol) and ethyl polyphosphate (PPE, 1 mL/0.05 g) was refluxed for 5 h. After reaching room temperature, the resulting solution was extracted with water (5 × 6 mL). The aqueous phases were pooled, filtered, and made alkaline with 10% aqueous NaOH. The mixture was extracted with chloroform (3 × 15 mL). The organic phases were washed with water, dried over sodium sulfate, and filtered. The chloroformic solution was left at r.t. until no further conversion to compounds **1** was evidenced by TLC (silica gel, chloroform:methanol 9:1). The solvent was then removed in vacuo and the crude product was purified by column chromatography (silica gel, chloroform:methanol 10:0–9:1).

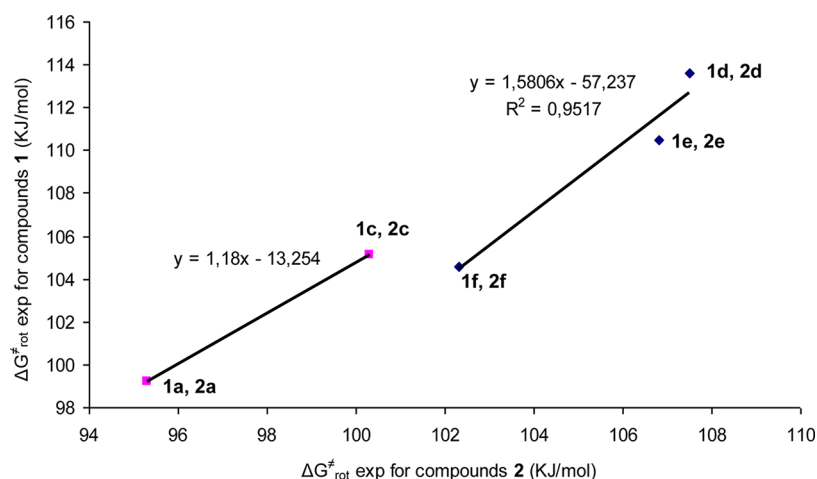


Figure 5. Rotational barriers of compounds containing 6- vs 5-membered amidine ring.

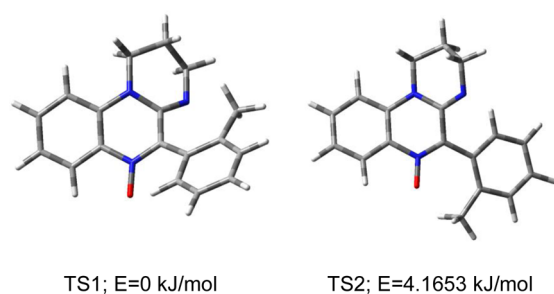


Figure 6. Transition states for the enantiomerization of compound 1a computed at the B3LYP/6-31+G(d,p) level.

Table 3. Calculated Rotational Barriers

compd	Ar	<i>n</i>	calculated barrier (kJ mol ⁻¹)	experimental barrier (kJ mol ⁻¹)
1a	2-CH ₃ C ₆ H ₄	1	88.3	99.2 99.8
1b	2-NO ₂ C ₆ H ₄	1	84.7	87.1
1c	1-C ₁₀ H ₇	1	89.1	105.1
1e	2-BrC ₆ H ₄	1	105.3	110.1
1f	2-ClC ₆ H ₄	1	96.7	104.6
1g	2-FC ₆ H ₄	1	67.7	81.5
2a	2-CH ₃ C ₆ H ₄	0	86.7	95.3
2c	1-C ₁₀ H ₇	0	86.1	100.3 100.3
2e	2-BrC ₆ H ₄	0	105.5	106.8
2f	2-ClC ₆ H ₄	0	96.0	102.3 101.2

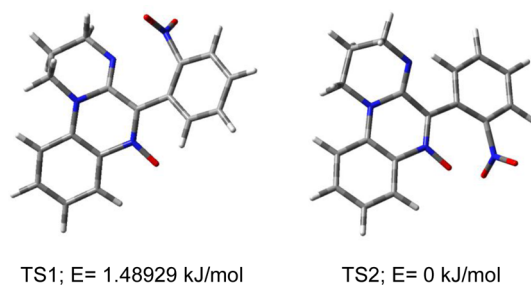


Figure 7. Transition states for the enantiomerization of compound 1b computed at the B3LYP/6-31+G(d,p) level.

Compounds 1a,⁶ 1d,⁸ 1e,⁶ and 2a,⁶ were described in the literature. Yields and analytical data of new compounds are as follows.

5-(2-Nitrophenyl)-2,3-dihydro-1H-pyrimido[1,2-*a*]quinoxaline 6-oxide 1b (0.155 g, 48%): mp 174–176 °C. ¹H NMR (500 MHz, CDCl₃): δ 2.02–2.06 (2H, m), 3.47–3.57 (2H, m), 3.87–3.96 (2H, m), 7.14 (1H, d, *J* = 8.5), 7.20–7.23 (1H, m), 7.55–7.58 (1H, m), 7.63–7.64 (2H, m), 7.78 (1H, t, *J* = 7.6), 8.24 (1H, d, *J* = 8.5), 8.36 (1H, d, *J* = 8.2). ¹³C NMR (500 MHz, CDCl₃): δ 19.5, 43.6, 44.0, 111.2, 121.1, 122.0, 124.5, 126.0, 130.0, 130.2, 131.7, 132.0, 133.8, 135.1, 136.1, 144.5, 148.3. HRMS (ESI) *m/z* calcd for C₁₇H₁₄N₄O₃: 322.1066. Found: 322.1070.

5-(Naphthalen-1-yl)-2,3-dihydro-1H-pyrimido[1,2-*a*]quinoxaline 6-oxide 1c (0.101 g, 31%): mp 186–188 °C. ¹H NMR (500 MHz, CDCl₃): δ 2.02–2.11 (2H, m), 3.47–3.59 (2H, m), 3.99 (2H, t, *J* = 6.1), 7.21–7.27 (2H, m), 7.44–7.50 (2H, m), 7.56–7.63 (4H, m), 7.91 (1H, d, *J* = 8.3), 7.96 (1H, d, *J* = 8.1), 8.41 (1H, dd, *J* = 8.1, 1.5). ¹³C NMR (500 MHz, CDCl₃): δ 19.2, 43.1, 44.2, 112.2, 121.4, 123.2, 124.3, 125.7, 126.2, 126.5, 126.9, 128.5, 129.0, 130.4, 130.5, 130.9, 132.4, 133.8, 134.7, 138.8, 146.4. HRMS (ESI) *m/z* calcd for C₂₁H₁₇N₃O: 327.1372. Found: 327.1368.

5-(2-Fluorophenyl)-2,3-dihydro-1H-pyrimido[1,2-*a*]quinoxaline 6-oxide 1g (0.139 g, 47%): mp 168–170 °C. ¹H NMR (500 MHz, CDCl₃): δ 2.14 (2H, bs), 3.67 (2H, bs), 4.01 (2H, bs), 7.21–7.34 (4H, m), 7.48–7.52 (2H, m), 7.61 (1H, t, *J* = 7.9), 8.41 (1H, d, *J* = 8.2). ¹³C NMR (500 MHz, CDCl₃): δ 19.5, 43.8, 44.0, 111.2, 116.0 (*J* = 21.5), 117.8 (*J* = 14.7), 121.3, 122.2, 124.15, 130.4, 131.6 (*J* = 2.9), 131.6 (*J* = 9.8), 132.1, 135.1, 136.6, 145.0, 160.2 (*J* = 249.4). HRMS (ESI) *m/z* calcd for C₁₇H₁₄FN₃O: 295.1121. Found: 295.1124.

4-(Naphthalen-1-yl)-1,2-dihydroimidazo[1,2-*a*]quinoxaline 5-oxide 2c (0.141 g, 45%): mp 100–102 °C. ¹H NMR (500 MHz, CDCl₃): δ 4.10–4.24 (4H, m), 6.90 (1H, dd, *J* = 8.1, 1.0), 7.15–7.18 (1H, m), 7.49–7.59 (4H, m), 7.62–7.65 (1H, m), 7.72 (1H, dd, *J* = 7.1, 1.1), 7.92–7.95 (1H, m), 8.01 (1H, d, *J* = 8.2), 8.32 (1H, dd, *J* = 8.3, 1.3). ¹³C NMR (500 MHz, CDCl₃): δ 46.6, 54.2, 112.0, 121.2, 121.4, 124.8, 125.4, 126.1, 126.5, 126.8, 128.3, 128.9, 130.0, 130.7, 131.0, 132.4, 133.6, 133.7, 136.3, 153.5. HRMS (ESI) *m/z* calcd for C₂₀H₁₅N₃O: 313.1215. Found: 313.1219.

4-(2-Iodophenyl)-1,2-dihydroimidazo[1,2-*a*]quinoxaline 5-oxide 2d (0.175 g, 45%): mp 139–141 °C. ¹H NMR (500 MHz, CDCl₃): δ 4.06–4.19 (2H, m), 4.19–4.23 (2H, m), 6.87 (1H, dd, *J* = 8.1, 1.1), 7.15 (1H, ddd, *J* = 8.3, 7.3, 1.1), 7.20 (1H, ddd, *J* = 8.0, 7.6, 1.6), 7.40 (1H, dd, *J* = 7.9, 1.6), 7.51–7.54 (1H, m), 7.54–7.56 (1H, m), 7.99 (1H, dd, *J* = 8.0, 0.9), 8.30 (1H, dd, *J* = 8.3, 1.1). ¹³C NMR (500 MHz, CDCl₃): δ 46.5, 53.9, 97.5, 112.2, 121.4, 121.4, 128.6, 130.7, 131.1, 131.1, 132.6, 133.5, 134.6, 138.0, 139.3, 152.4. HRMS (ESI) *m/z* calcd for C₁₆H₁₂IN₃O: 389.0025. Found: 389.0030.

4-(2-Chlorophenyl)-1,2-dihydroimidazo[1,2-*a*]quinoxaline 5-oxide 2f (0.119 g, 40%): mp 170–172 °C. ¹H NMR (500 MHz, CDCl₃): δ 4.08–4.26 (4H, m), 6.87 (1H, dd, *J* = 8.1, 1.1), 7.15 (1H, ddd, *J* =

8.3, 7.3, 1.1), 7.42–7.47 (2H, m), 7.49–7.57 (3H, m), 8.30 (1H, dd, $J = 8.3, 1.3$). ^{13}C NMR (500 MHz, CDCl_3): δ 46.5, 54.3, 112.0, 121.1, 121.3, 127.1, 128.3, 129.9, 130.8, 130.8, 130.9, 131.1, 132.5, 133.6, 134.1, 152.6. HRMS (ESI) m/z calcd for $\text{C}_{16}\text{H}_{12}\text{ClN}_3\text{O}$: 297.0669. Found: 297.0665.

Synthesis of *N*-arylacetyl-*N'*-(2-nitroaryl)-1,3-propanediamines **3** and *N*-arylacetyl-*N'*-(2-nitroaryl)-1,2-ethanodiamines **4**. General Procedure: The acyl chloride (1 mmol) was added to a chloroformic solution of the corresponding *N*-(*o*-nitrophenyl)-1,*n*-diamine (1 mmol), followed by aq 4% NaOH (1 mL). The mixture was shaken for 15 min, after which the organic layer was separated, washed with H_2O , dried (Na_2SO_4), and filtered. The solvent was removed in vacuo. The crude product was purified by flash chromatography on silica gel using mixtures of chloroform:ethyl acetate as eluent.

Compounds **3a**, **6d**, **8e**, **f** and **4a**, **e** were described in the literature. Yields and analytical data of new compounds are as follows.

N-(2-Nitrophenyl)acetyl-*N'*-(2-nitrophenyl)-1,3-propanediamine **3b** (0.283 g, 79%): mp 148–150 °C. ^1H NMR (500 MHz, CDCl_3): δ 1.93–1.99 (2H, m), 3.38 (2H, t, $J = 6.8$), 3.44–3.47 (2H, m), 3.88 (2H, s), 6.04 (1H, bs, ex), 6.66–6.69 (1H, m), 6.86 (1H, d, $J = 8.5$), 7.39–7.53 (3H, m), 7.64 (1H, t, $J = 7.6$), 8.06 (1H, d, $J = 8.2$), 8.19 (1H, d, $J = 8.7$). ^{13}C NMR (500 MHz, CDCl_3): δ 29.1, 37.6, 40.5, 41.1, 113.7, 115.4, 125.2, 126.9, 128.5, 130.3, 130.6, 133.5, 133.7, 136.3, 145.3, 169.4. HRMS (ESI) m/z calcd for $\text{C}_{17}\text{H}_{18}\text{N}_4\text{O}_5$: 358.1277. Found: 358.1279.

N-(1-Naphthyl)acetyl-*N'*-(2-nitrophenyl)-1,3-propanediamine **3c** (0.280 g, 77%): mp 132–134 °C. ^1H NMR (500 MHz, CDCl_3): δ 1.71–1.76 (2H, m), 3.06–3.12 (2H, m), 3.28 (2H, c, $J = 6.4$), 4.04 (2H, s), 5.45 (1H, bs, ex), 6.56 (1H, dd, $J = 8.7, 0.8$), 6.62 (1H, dd, $J = 8.5, 7.1$), 7.32–7.56 (5H, m), 7.81–7.97 (3H, m), 8.13 (1H, dd, $J = 8.5, 1.5$). ^{13}C NMR (500 MHz, CDCl_3): δ 28.8, 37.2, 40.2, 41.8, 113.5, 115.3, 123.6, 125.4, 125.7, 126.2, 126.3, 126.8, 128.4, 128.6, 128.8, 130.9, 131.9, 133.9, 136.1, 145.2, 171.4. HRMS (ESI) m/z calcd for $\text{C}_{21}\text{H}_{21}\text{N}_3\text{O}_5$: 363.1583. Found: 363.1579.

N-(2-Fluorophenyl)acetyl-*N'*-(2-nitrophenyl)-1,3-propanediamine **3g** (0.271 g, 82%): mp 121–125 °C. ^1H NMR (500 MHz, CDCl_3): δ 1.87–1.92 (2H, m), 3.30–3.34 (2H, m), 3.37–3.41 (2H, m), 3.60 (2H, s), 6.02 (1H, bs, ex), 6.64 (1H, ddd, $J = 8.5, 7.0, 1.4$), 6.80 (1H, d, $J = 8.0$), 7.04–7.08 (1H, m), 7.11–7.14 (2H, m), 7.25–7.33 (2H, m), 7.40–7.43 (1H, m), 8.06 (1H, bs, ex), 8.14 (1H, dd, $J = 8.7, 1.4$). ^{13}C NMR (500 MHz, CDCl_3): δ 28.9, 36.8 ($J = 2.7$), 37.3, 40.3, 113.6, 115.3, 115.5 ($J = 21.8$), 121.5 ($J = 15.4$), 124.5 ($J = 3.6$), 126.8, 129.2 ($J = 8.2$), 131.6 ($J = 3.6$), 131.8, 136.2, 145.2, 160.8 ($J = 245.2$), 170.2. HRMS (ESI) m/z calcd for $\text{C}_{17}\text{H}_{18}\text{FN}_3\text{O}_5$: 331.1332. Found: 331.1335.

N-(1-Naphthyl)acetyl-*N'*-(2-nitrophenyl)ethylenediamine **4c** (oil, 0.283 g, 81%): ^1H NMR (500 MHz, CDCl_3): δ 3.30–3.45 (4H, m), 4.05 (2H, s), 5.60 (1H, bs, ex), 6.61–6.62 (1H, m), 6.87 (1H, d, $J = 7.4$), 6.91–7.46 (5H, m), 7.81–7.87 (3H, m), 8.16 (1H, dd, $J = 8.6, 1.7$). ^{13}C NMR (500 MHz, CDCl_3): δ 38.7, 41.6, 41.9, 113.6, 115.6, 123.5, 125.6, 126.2, 126.8, 126.8, 128.4, 128.6, 128.8, 130.6, 131.9, 132.0, 133.9, 136.3, 145.2, 171.7. HRMS (ESI) m/z calcd for $\text{C}_{20}\text{H}_{19}\text{N}_3\text{O}_5$: 349.1426. Found: 349.1430.

N-(2-Iodophenyl)acetyl-*N'*-(2-nitrophenyl)ethylenediamine **4d** (0.395 g, 93%): mp 143–145 °C. ^1H NMR (500 MHz, CDCl_3): δ 3.53–3.54 (4H, m), 3.75 (2H, s), 5.83 (1H, bs, ex), 6.68 (1H, dd, $J = 8.5, 7.0$), 6.97 (1H, dd, $J = 8.6, 1.0$), 7.00 (1H, ddd, $J = 8.0, 6.7, 2.4$), 7.32–7.37 (2H, m), 7.44–7.47 (1H, m), 7.86 (1H, dd, $J = 8.0, 0.8$), 8.10 (1H, bs, ex), 8.17 (1H, dd, $J = 8.5, 1.4$). ^{13}C NMR (500 MHz, CDCl_3): δ 38.8, 41.9, 48.5, 101.1, 113.7, 115.7, 126.9, 128.9, 129.3, 130.9, 132.1, 136.4, 137.9, 139.9, 145.2, 170.2. HRMS (ESI) m/z calcd for $\text{C}_{16}\text{H}_{16}\text{IN}_3\text{O}_5$: 425.0236. Found: 425.0231.

N-(2-Chlorophenyl)acetyl-*N'*-(2-nitrophenyl)ethylenediamine **4f** (0.253 g, 76%): mp 93–99 °C. ^1H NMR (500 MHz, CDCl_3): δ 3.47–3.52 (4H, m), 3.71 (2H, s), 5.80 (1H, bs, ex), 6.64–6.69 (1H, m), 6.94 (1H, dd, $J = 8.7, 1.0$), 7.22–7.46 (5H, m), 8.05 (1H, bs, ex), 8.16 (1H, dd, $J = 8.7, 1.5$). ^{13}C NMR (500 MHz, CDCl_3): δ 38.9, 41.4, 41.9, 113.7, 115.7, 126.8, 127.4, 129.1, 129.8, 131.7, 132.1, 132.6, 134.3, 136.3, 145.2, 170.5. HRMS (ESI) m/z calcd for $\text{C}_{16}\text{H}_{16}\text{ClN}_3\text{O}_5$: 333.0880. Found: 333.0882.

■ ASSOCIATED CONTENT

Supporting Information

^1H and ^{13}C NMR spectra for compounds **1b,c,g**, **2c,d,f**, **3b,c,g**, and **4c,d,f**, chiral HPLC screening for compounds **1b–c** and **2a,c,f**, kinetic data for racemization for compounds **1a,c,f**, **2c–f**, computational details, crystallographic data, and X-ray crystallographic file (CIF) for compound **1a**. This material is available free of charge via the Internet at <http://pubs.acs.org>.

■ AUTHOR INFORMATION

Corresponding Authors

*E-mail: christian.roussel@univ-amu.fr.

*E-mail: lorelli@ffyba.uba.ar.

Notes

The authors declare no competing financial interest.

■ ACKNOWLEDGMENTS

This work was supported by the University of Buenos Aires (20020100100935) and by CONICET (PIP 286).

■ REFERENCES

- (1) Adams, G. E.; Fielden, E. M.; Naylor, M. A.; Stratford, I. J. U.K. Pat. Appl. GB 2257360, 1993.
- (2) Parthasarathy, P. C.; Joshi, B. S.; Chaphekar, M. R.; Gawad, D. H.; Anandan, L.; Likhate, M. A.; Hendi, M.; Mudaliar, S.; Iyer, S.; Ray, D. K.; Srivastava, V. B. *Indian J. Chem., Sect. B* **1983**, *22*, 1250.
- (3) Ellames, G. J.; Lawson, K. R.; Jaxa-Chamiec, A. A.; Upton, R. M. European Patent no. EP 0256545, 1988.
- (4) García, M. B.; Orelli, L. R.; Magri, M. L.; Perillo, I. A. *Synthesis* **2002**, 2687.
- (5) García, M. B.; Orelli, L. R.; Perillo, I. A. *J. Heterocycl. Chem.* **2006**, *43*, 1703.
- (6) Díaz, J. E.; García, M. B.; Orelli, L. R. *J. Mol. Struct.* **2010**, *982*, 50.
- (7) Lavaggi, M. L.; Aguirre, G.; Boiani, L.; Orelli, L. R.; García, M. B.; Cerecetto, H.; González, M. *Eur. J. Med. Chem.* **2008**, *43*, 1737.
- (8) Gruber, N.; Piehl, L. L.; Rubin de Celis, E.; Díaz, J. E.; García, M. B.; Stipa, P.; Orelli, L. R. *RSC Adv.* **2015**, *5*, 2724.
- (9) (a) Manschreck, A.; Koller, H.; Stühler, G.; Davies, M. A.; Traber, J. *Eur. J. Med. Chem. Chim. Therap.* **1984**, *19*, 381. (b) Chenard, B. L.; Welch, W. M. US Patent 6,323,208, 2001. (c) Chenard, B. L.; Devries, K. M.; Welch, W. M. US Patent 6,380,204, 2002. (d) Bach, F. L.; Barclay, J. C.; Kende, F.; Cohen, E. *J. Med. Chem.* **1968**, *11*, 987. (e) Orton, T. C.; Adam, H. K.; Bentley, M.; Holloway, B.; Tucker, M. *J. Toxicol. Appl. Pharmacol.* **1984**, *73*, 138. (f) Brunner, F.; Zini, R.; Tillement, J. P. *Int. J. Clin. Pharmacol. Therap. Toxicol.* **1984**, *22*, 134. (g) Lackner, T. E.; Clissold, S. P. *Drugs* **1989**, *38*, 204. (h) Chiladakis, I.; Hindricks, G.; Haverkamp, W.; Vogt, J.; Guelker, H. *Arzneim.-Forsch.* **1989**, *39*, 1130. (i) Drewe, J.; Narjes, H.; Heinzl, G.; Brickl, R.-S.; Rohr, A.; Beglinger, C. *Br. J. Clin. Pharmacol.* **2000**, *50*, 69. (j) Leroux, F.; Hutschenreuter, T. U.; Charrière, C.; Scopelliti, R.; Hartmann, R. W. *Helv. Chim. Acta* **2003**, *86*, 2671. (k) Shinkai, N.; Korenaga, K.; Takizawa, H.; Mizu, H.; Yamauchi, H. *J. Pharm. Pharmacol.* **2008**, *60*, 71. (l) Kozak, W.; Kozak, A.; Johnson, M. H.; Elewa, H. F.; Fagan, S. C. *J. Pharmacol. Exp. Therap.* **2008**, *326*, 773.
- (10) (a) Upadhyay, S. P.; Pissurlenkar, R. R. S.; Coutinho, E. C.; Karnik, A. V. *J. Org. Chem.* **2007**, *72*, 5709. (b) Kim, K. S.; Jun, E. J.; Kim, S. K.; Choi, H. J.; Yoo, J.; Lee, C.-H.; Hyun, M. H.; Yoon, J. *Tetrahedron Lett.* **2007**, *48*, 2481.
- (11) Bringmann, G.; Günther, C.; Ochse, M.; Schupp, O.; Tasler, S. *Prog. Chem. Org. Natl. Prod.* **2001**, *82*, 1.
- (12) Among others: (a) Hayashi, T. *Catal. Surveys Jpn.* **1999**, *3*, 127. (b) Ojima, I. *Catalytic Asymmetric Synthesis*; Wiley: New York, 2000. (c) Ohkuma, T.; Noyori, R. *Comprehensive Asymmetric Cat. (Suppl. 1)* **2004**. (d) Bringmann, G.; Menche, D. *Acc. Chem. Res.* **2001**, *34*, 615. and reference 5 therein. (e) Buchwald, S. L.; Mauger, C.; Mignani, G.; Scholz, U. *Adv. Synth. Catal.* **2006**, *348*, 23. (f) Hartwig, J. F. *Synlett*

2006, 1283. (g) Roseblade, S. J.; Pfaltz, A. *Acc. Chem. Res.* **2007**, *40*, 1402.

(13) Alkorta, I.; Elguero, J.; Roussel, C.; Vanthuyne, N.; Piras, P. *Adv. Heterocycl. Chem.* **2012**, *105*, 1.

(14) Sandström, J. *Dynamic NMR Spectroscopy*; Academic Press: London, 1982; Chapter 6.

(15) (a) Najahi, E.; Vanthuyne, N.; Nepveu, F.; Jean, M.; Alkorta, I.; Elguero, J.; Roussel, C. *J. Org. Chem.* **2013**, *78*, 12577. (b) Roussel, C.; Vanthuyne, N.; Boucekara, M.; Djafri, A.; Elguero, J.; Alkorta, I. *J. Org. Chem.* **2008**, *73*, 403.

(16) (a) García, M. B.; Grilli, S.; Lunazzi, L.; Mazzanti, A.; Orelli, L. *J. Org. Chem.* **2001**, *66*, 6679. (b) García, M. B.; Grilli, S.; Lunazzi, L.; Mazzanti, A.; Orelli, L. *Eur. J. Org. Chem.* **2002**, *23*, 4018. (c) Magri, M. L.; Vanthuyne, N.; Roussel, C.; García, M. B.; Orelli, L. *J. Chromatogr., A* **2005**, *1069*, 203. (d) Díaz, J. E.; Gruber, N.; Lunazzi, L.; Mazzanti, A.; Orelli, L. *Tetrahedron* **2011**, *67*, 9129.

(17) Bryce, T. A.; Maxwell, J. R. *Chem. Commun.* **1965**, 206.

(18) Tatematsu, A.; Yoshizumi, H. *Tetrahedron Lett.* **1967**, *31*, 2985.

(19) Wolf, C. *Chem. Soc. Rev.* **2005**, *34*, 595.

(20) (a) Roussel, C.; Adjimi, M.; Chemlal, A.; Djafri, A. *J. Org. Chem.* **1988**, *53*, 5076. (b) Tambuté, A.; Siret, L.; Begos, A.; Caude, M. *Chirality* **1992**, *4*, 36. (c) Roussel, C.; Lehuédé, S.; Popescu, C.; Stein, J.-L. *Chirality* **1993**, *5*, 207. (d) Pirkle, W. H.; Welch, C. J. *Tetrahedron: Asymmetry* **1994**, *5*, 777. (e) Pirkle, W. H.; Koscho, M. E.; Wu, Z. *J. Chromatogr., A* **1996**, *726*, 91. (f) Roussel, C.; Hart, N.; Bonnet, B.; Suteu, C.; Hirtopeanu, A.; Kravtsov, V. C.; Luboradzki, R.; Vanthuyne, N. *Chirality* **2002**, *14*, 665. (g) Hirtopeanu, A.; Suteu, C.; Uncuta, C.; Mihai, G.; Roussel, C. *Eur. J. Org. Chem.* **2000**, 1081. (h) Roussel, C.; Suteu, C. *Enantiomer* **1997**, *2*, 449. (i) Roussel, C.; Bonnet, B.; Piederriere, A.; Suteu, C. *Chirality* **2001**, *13*, 56. (j) Wolf, C.; Pirkle, W. H. *J. Chromatogr., A* **1998**, *799*, 177. (k) Pirkle, W. H.; Brice, J.; Terfloth, G. J. *J. Chromatogr., A* **1996**, *753*, 109. (l) Fujita, M.; Kitagawa, O.; Yamada, Y.; Izawa, H.; Hasegawa, H.; Taguchi, T. *J. Org. Chem.* **2000**, *65*, 1108. (m) Godfrey, C. R. A.; Simpkins, N. S.; Walker, M. D. *Synlett* **2000**, *3*, 388. (n) Oguz, F. S.; Berg, U.; Dogan, I. *Enantiomer* **2000**, *5*, 405. (o) Oguz, F. S.; Dogan, I. *Tetrahedron: Asymmetry* **2003**, *14*, 1857. (p) Sakamoto, M.; Shigekura, M.; Saito, A.; Ohtake, T.; Mino, T.; Fujita, T. *Chem. Commun.* **2003**, 2218. (q) Ordu, O. D.; Dogan, I. *Tetrahedron: Asymmetry* **2004**, *15*, 925. (r) Demir-Ordu, O.; Yilmaz, E. M.; Dogan, I. *Tetrahedron: Asymmetry* **2005**, *16*, 3752. (s) Sakamoto, M.; Utsumi, N.; Ando, M.; Saeki, M.; Mino, T.; Fujita, T.; Katoh, A.; Nishio, T.; Kashima, C. *Angew. Chem., Int. Ed.* **2003**, *42*, 4360. (t) Dogan, H.; Pustet, N.; Mannschreck, A. *J. Chem. Soc., Perkin Trans. 2* **1993**, 1557.

(21) Trapp, O.; Schurig, V. *Chirality* **2002**, *14*, 465.

(22) (a) Ruzziconi, R.; Spizzichino, S.; Lunazzi, L.; Mazzanti, A.; Schlosser, M. *Chem.—Eur. J.* **2009**, *15*, 2645. (b) Mazzanti, A.; Lunazzi, L.; Ruzziconi, R.; Spizzichino, S.; Schlosser, M. *Chem.—Eur. J.* **2010**, *16*, 9186. (c) Lunazzi, L.; Mancinelli, M.; Mazzanti, A.; Lepri, S.; Ruzziconi, R.; Schlosser, M. *Org. Biomol. Chem.* **2012**, *10*, 1847.

(23) Perillo, I.; Fernandez, B.; Lamdan, S. *J. Chem. Soc., Perkin Trans.* **1977**, 2068.

(24) (a) The basic site in cyclic amidines is the formally sp² nitrogen atom, due to resonance stabilization of the resulting amidinium cation. (b) Reported pK_A values for 1-phenyl-2-(4-nitrophenyl)imidazoline: 7.65 and for 1-phenyl-2-(4-nitrophenyl)-1,4,5,6-tetrahydropyrimidine: 10.51 (taken from ref 23).

(25) (a) Yap, G. P. A.; Alkorta, I.; Jagerovic, N.; Elguero, J. *Aust. J. Chem.* **2004**, *57*, 1103. (b) Yap, G. P. A.; Jové, F. A.; Claramunt, R. M.; Sanz, D.; Alkorta, I.; Elguero, J. *Aust. J. Chem.* **2004**, *58*, 817. (c) O'Leary, J.; Wallis, J. D. *CrystEngComm* **2007**, *9*, 941. (d) Chiarucci, M.; Ciogli, A.; Mancinelli, M.; Ranieri, S.; Mazzanti, A. *Angew. Chem.* **2014**, *126*, 5509.